

Composite membranes of chitosan and titania-coated carbon nanotubes as promising materials for new proton-exchange membranes

Hai Liu,¹ Jie Wang,² Sheng Wen,¹ Chunli Gong,¹ Fan Cheng,¹ Guangjin Wang,¹ Genwen Zheng,¹ Caiqin Qin¹

¹Faculty of Chemistry and Material Science, Hubei Engineering University, Xiaogan, Hubei 432000, China

²School of Materials Science and Engineering, Wuhan University of Technology, Wuhan, Hubei 430072, China

Correspondence to: H. Liu (E-mail: wjlh804@gmail.com)

ABSTRACT: Titania-coated carbon nanotubes (TCNTs) were obtained by a simple sol–gel method. Then chitosan/TCNT (CS/TCNT) composite membranes were prepared by stirring chitosan/acetic acid and a TCNT/ethanol suspension. The morphology, thermal and oxidative stabilities, water uptake and proton conductivity, and mechanical properties of CS/TCNT composite membranes were investigated. The CNTs coated with an insulated and hydrophilic titania layer eliminated the risk of electronic short-circuiting. Moreover, the titania layer enhanced the interaction between TCNTs and chitosan to ensure the homogenous dispersion of TCNTs in the chitosan matrix. The water uptake of CS/TCNT composite membranes was reduced owing to the decrease of the effective number of the $-\text{NH}_2$ functional groups of chitosan. However, the CS/TCNT composite membranes exhibited better performance than a pure CS membrane in thermal and oxidative stability, proton conductivity, and mechanical properties. These results suggest that CS/TCNT composite membranes are promising materials for new proton-exchange membranes. © 2016 Wiley Periodicals, Inc. *J. Appl. Polym. Sci.* 2016, 133, 43365.

KEYWORDS: mechanical properties; membranes; morphology; thermal properties

Received 10 September 2015; accepted 20 December 2015

DOI: 10.1002/app.43365

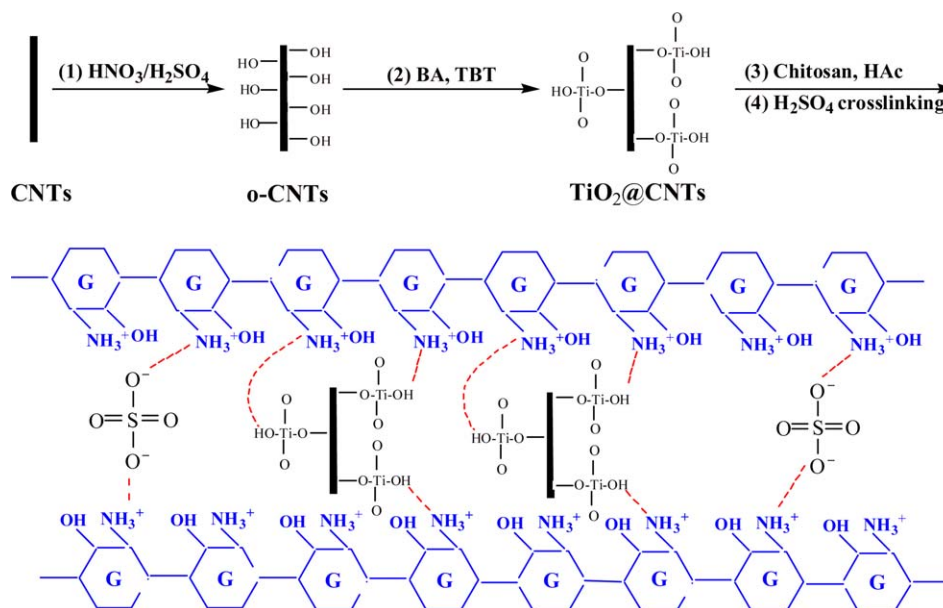
INTRODUCTION

Fuel cells are the most suitable energy source for portable devices and vehicles because of their high energy conversion efficiency and relatively low operation temperature. As a core component in fuel cells, a proton-exchange membrane (PEM) is a medium transferring protons and a barrier preventing direct contact of fuel and oxidant. In recent decades, extensive research on the development of high-performance fuel cells has been done in order to generate and store energy at low cost. Cost-effective and environmentally friendly PEMs prepared from natural polymers will become a promising substitute for currently used synthetic polymers such as Nafion and sulfonated engineering polymers.^{1–3}

Chitosan (CS) is the partially deacetylated polysaccharide of chitin that is the principal component of living organisms such as fungi and crustaceans. It has attracted more attention because it has excellent biocompatibility and biodegradability, high hydrophilicity, low methanol permeability, and easy chemical functionalization.⁴ In the past few years, CS has been extensively studied as a membrane material for separation, reverse osmosis,

ultrafiltration, and polymer electrolyte-based fuel cells.^{5–7} In its natural state, CS has very low proton conductivity owing to no mobile protons in its structure. It cannot be directly used as a PEM. Many modification methods, including sulfonation, phosphorylation, chemical crosslinking, inorganic particle filling modification, and blending with other polymers, have been applied to improve the proton conductivity of CS-based PEMs.^{8–10} However, the relatively poor mechanical and electrical properties of CS restrict its wide applications. Development of organic–inorganic composite membranes is a feasible and effective way to solve the above problems because the inorganic component can increase the mechanical and thermal stability of the composites while suppressing methanol crossover.⁹

Carbon nanotubes (CNTs) have been widely recognized as multifunctional components of next-generation composite materials owing to their extraordinary electrical, thermal, optical, and mechanical properties.^{11,12} However, the addition of CNTs into PEMs was not ever under consideration for two reasons. One is CNTs can form electronic channels in PEMs and hence lead to the risk of short-circuiting in fuel cells due to the excellent electrical conductivity of CNTs with a graphite wall structure.



Scheme 1. Preparation of CS/TCNT composite membranes. [Color figure can be viewed in the online issue, which is available at wileyonlinelibrary.com.]

Another is CNTs are poorly dispersed in a polymer matrix because of the strong intrinsic Van der Waals forces among the tubes. In order to overcome the bottleneck of CNTs used in PEMs, some functionalized CNTs, such as carboxylic acid–functionalized CNTs, sulfonated CNTs, phosphonated CNTs, and Nafion- and polybenzimidazole-functionalized CNTs, have been used as inorganic components to modify PEMs.^{13–16}

In this work, TiO₂-coated CNTs (TCNTs) were prepared by a simple sol–gel method. The as-prepared TCNTs could effectively prohibit electron conduction through the composite membranes. For this reason, a series of chitosan/TCNT (CS/TCNT) composite membranes were successfully fabricated by a solution casting method and subsequently a chemical crosslinking process with sulfuric acid. The morphology of TCNTs and the physicochemical properties of CS/TCNT composite membranes were investigated.

EXPERIMENTAL

Materials

Chitosan with a 92.5% degree of deacetylation was supplied by Golden-shell Biochemical Co. (China, Taizhou). Multiwalled CNTs (chemical vapor deposition method, diameter: 40–60 nm, length: 5–15 μm , purity >95%) were purchased from Shenzhen Nanotech Port Co. (China, Shenzhen). Tetrabutyl titanate (TBT) was provided by Tianjin Bodi Chemical Co. (China, Tianjin). Sulfuric acid (98%) and nitric acid (65%) were purchased from Kaifeng Shenma Group Co. (China, Kaifeng) and Hengxin chemical reagent factory (China, Shanghai), respectively. Acetic acid (analytical reagent, AR), *N,N*-dimethylacetamide (DMAc, AR), and ammonia (AR) were all purchased from Sinopharm Chemical Reagent Co. (China, Shanghai).

Preparation of TCNTs

The pristine CNTs were pretreated in a mixture of concentrated HNO₃ and H₂SO₄ (volume ratio 3:1) at 100°C for 6 h, followed by thorough washing with distilled water until the filtrate

became neutral. The solid was then resuspended in HCl for 12 h at 100°C. The suspension was finally vacuum-filtered with a 0.22 μm polyamide membrane and dried under vacuum for 10 h at 100°C to yield oxidized CNTs. The oxidized CNTs were ultrasonically dispersed in a mixture of anhydrous ethanol, benzyl alcohol, and distilled water with a volume ratio of 4:1:2 for 0.5 h. Then, TBT was added quickly, and the mixture was held for 2 h under stirring at room temperature. The resultant sediment was ultrasonically redispersed in ethanol for 0.25 h, then vacuum-filtered with a 0.22 μm polyamide membrane. The same procedure was repeated at least three times. The resultant product was gradually dried in air and finally kept in a vacuum oven at 60°C for 10 h.

Preparation of CS/TCNT Composite Membranes

Typical CS/TCNT composite membranes were prepared as follows. A desired amount of TCNTs was ultrasonically dispersed in ethanol for 30 min at room temperature. Then, the TCNT/ethanol suspension was added to the 2 wt % chitosan/acetic acid solution. The above two solutions were uniformly mixed by ultrasonic oscillation. The bubbles were removed, and then the composite membranes were formed by a solution casting method. The resultant composite membranes were finally soaked in a 0.5 mol L⁻¹ sulfuric acid solution for crosslinking. The composite membranes with various TCNT contents (0 wt %, 1 wt %, 2 wt %, 5 wt %, and 10 wt %) were named CS/TCNTs-0, CS/TCNTs-1, CS/TCNTs-2, CS/TCNTs-5, and CS/TCNTs-10, respectively. The complete process for CS/TCNT composite membrane preparation is presented in Scheme 1.

Measurements and Characterization

The morphology of TCNTs was observed by transmission electron microscopy (TEM, FEI Co., Netherlands, Eindhoven) at an accelerating voltage of 200 kV by dispersing the material in ethanol, placing a few drops of the dispersion on a copper grid, and evaporating them prior to observation.

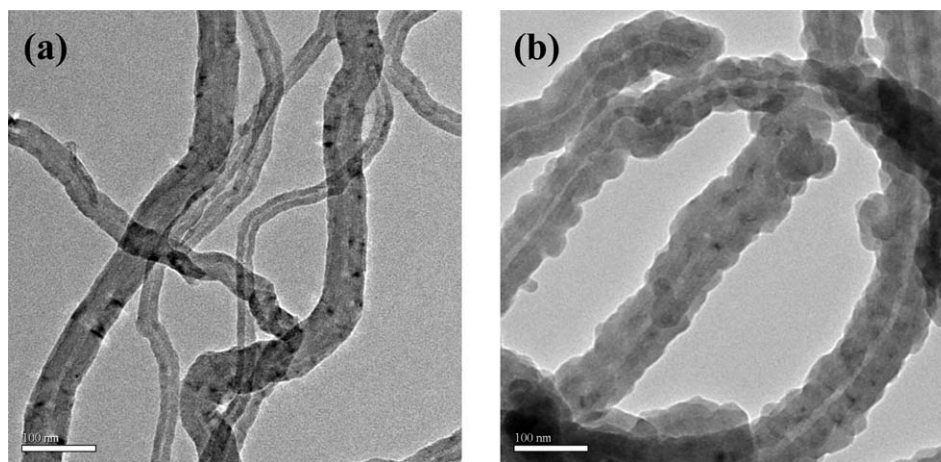


Figure 1. TEM images of (a) oxidized CNTs and (b) TiO₂-coated CNTs.

The Fourier transform infrared (FTIR) spectra were recorded by using a Thermo Nicolet Nexus spectrometer (Thermo Nicolet, America, Madison) between 4000 cm⁻¹ and 400 cm⁻¹ with a resolution of 2 cm⁻¹ at room temperature.

The cross-sectional morphology of the CS/TCNT composite membranes was examined using an SEM (X-650, Hitachi Co., Japan, Tokyo). The membranes were fractured by brief immersion in liquid nitrogen. Fresh cross-sectional cryogenic fractures of the membranes were vacuum-sputtered with a thin layer of Pt/Pd before analysis.

Thermogravimetric analyses were performed on CS/TCNT composite membranes by measuring the change in the weight of the samples as the temperature was increased by using thermogravimetric analysis (TGA; SDT Q600, TA Co., America, New Castle). Initially, the samples were heated under nitrogen to 100°C for 10 min to remove the water absorbed in the samples, cooled down to 50°C, and then reheated to 800°C at a rate of 10°C min⁻¹ under a nitrogen atmosphere.

A small membrane sample with a thickness of 60 μm was soaked in Fenton's reagent (3% H₂O₂ with 2 ppm FeSO₄) at 80°C. The oxidation stability was evaluated by recording the time taken by the membranes to break themselves into pieces.

The composite membranes were dried in a vacuum oven at 100°C for 24 h, weighed (W_{dry}), and immersed in distilled water at different temperatures for 48 h. Then, the wet membranes were blotted to remove surface water droplets and quickly weighed (W_{wet}). The water uptake of membranes was calculated as follows:

$$\text{Water uptake (\%)} = \frac{W_{\text{wet}} - W_{\text{dry}}}{W_{\text{dry}}} \times 100\% \quad (1)$$

The proton conductivity of the composite membranes was measured using the AC impedance method. In a chamber, the tested membranes were put into a clamp and connected by two platinum electrodes to an electrochemical workstation (Autolab PGSTAT 302N, Switzerland, Herisau) with a frequency range of 100 Hz to 1 MHz and an AC voltage amplitude of 10 mV. Prior to testing, all membranes were hydrated by immersion in distilled water for 24 h at room temperature. A sample of prehy-

drated membrane (3 × 3 cm) was clamped between the two electrodes. The proton conductivity was calculated as follows:

$$\sigma = l/Rdw \quad (2)$$

where l is the distance between the electrodes, d and w are the thickness and width of the films, respectively, and R is the resistance value measured.

Tensile strength tests were performed according to the GB1040-2002 standard. The dumbbell specimens were measured with a universal tensile testing machine (AG-IC 5KN, Japan Shimadzu, Kyoto) at a crosshead speed of 2 mm/min at 20°C. The gauge length and width of the dumbbell specimens were 50 mm and 4 mm, respectively. At least three specimens were tested for each sample and then averaged.

RESULTS AND DISCUSSION

Morphology of TiO₂-Coated CNTs

The morphology of oxidized CNTs and oxidized CNTs coated with TiO₂ was directly observed by means of TEM. The pristine CNTs that we used are prepared by a chemical vapor deposition method, and there often exist some residual black catalyst particles. Figure 1(a) shows the TEM image of CNTs after oxidation treatment with concentrated acid. It can be seen that there are no obvious residual catalyst particles as well as a decrease in entanglement structure of the oxidized CNTs. After the sol-gel process, as compared with the smooth and clear surface of oxidized CNTs, the surface of the titania coating is rough because there are some nanoparticles attached to the surface of TCNTs. However, the thickness of the titania shell is relatively uniform. The formation of this thick TiO₂ layer may be related to chemical binding in which the surface functional groups (—COOH, —OH) of oxidized CNTs react with titanium hydroxide from the hydrolyzed TBT to form Ti—O—C linkages, and to a hydrogen-bonding interaction between titanium hydroxide and C=O groups on the CNT surface. In addition, these TiO₂ particles can also gather in the surface defects of oxidized CNTs and adsorb on the surface of oxidized CNTs. It can be expected that this thick and insulated TiO₂ coating layer on CNTs will increase the tunneling energy barrier and then effectively limit the intertube charge transport.^{17,18}

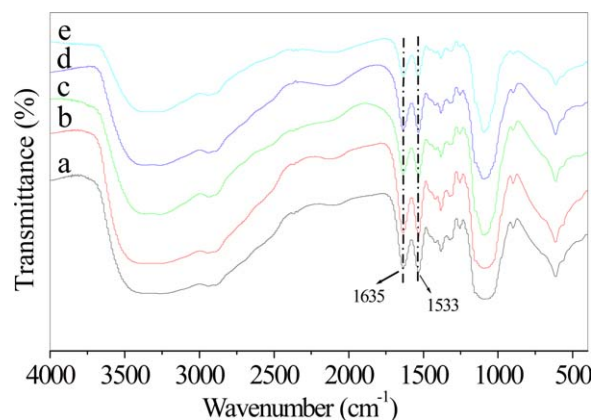


Figure 2. FTIR spectra of (a) CS/TCNTs-0, (b) CS/TCNTs-1, (c) CS/TCNTs-2, (d) CS/TCNTs-5 and (e) CS/TCNTs-10 composite membranes. [Color figure can be viewed in the online issue, which is available at wileyonlinelibrary.com.]

Structure and Morphology of CS/TCNT Composite Membranes

The molecular structures of CS/TCNT composite membranes were characterized by FTIR. The FTIR spectra of CS/TCNT composite membranes with TCNT content from 0 wt % to 10 wt % are shown in Figure 2. The CS/TCNT composite membranes exhibit similar FTIR absorption bands compared to the CS/TCNTs-0 membrane. In the curves of the CS/TCNT composite membranes, peaks appear at 1530 cm^{-1} and 1633 cm^{-1} , ascribed to the symmetric and asymmetric bending vibration of $-\text{NH}_3^+$, respectively.¹⁹ However, after the incorporation of TCNTs, the intensity of the $1635\text{--}1533\text{ cm}^{-1}$ band in the composite membranes decreases to a certain extent compared with those in the CS/TCNTs-0 membrane. This may be caused by two kinds of forces between chitosan and titania. One is electrostatic interactions between the positively charged ammonium groups of the chitosan backbone and the negatively charged $-\text{TiOH}$. The other is the hydrogen bonds between the $-\text{TiOH}$ groups and the surface of TCNTs and the $-\text{OH}$ or $-\text{NH}_2$ groups of chitosan.

The physical properties of the composite membranes largely depend on the dispersion of fillers in the polymer matrix.²⁰ In order to evaluate the dispersion of TCNTs in the CS matrix, the cross-sectional morphology of CS/TCNT composite membranes was observed by using SEM. The cross-sectional SEM micrographs of CS/TCNT composite membranes with different TCNT contents are shown in Figure 3(a–e). As can be seen from the figures, the pure CS membrane exhibits a homogeneous and void-free surface. With the addition of TCNTs, some obvious fibrous materials begin to appear in the cross section of the CS/TCNT composite membranes. Moreover, when the TCNT content increases, more and more fibrous materials can be observed in the cross section of CS/TCNT composite membranes [as seen in Figure 3(c–e)]. The TCNTs can uniformly disperse in the CS matrix without obvious aggregation [Figure 3(b,c,d)] when the added TCNT content is no more than 5 wt %. The uniform TCNT dispersion in the CS matrix may be related to the titania shell effectively avoiding tube–tube contacts and bundle formation. In addition, the hydrophilic titania coating layer may improve the compatibility of

the TCNTs and the CS matrix as compared with pristine CNTs. However, when the TCNT content reaches 10 wt %, the obvious aggregation of TCNTs can be found in the cross section of the CS/TCNT composite membrane [Figure 3(e)].

Thermal and Oxidative Stability of CS/TCNT Composite Membranes

The thermal stability of a PEM is a key property for its durability during fuel cell operation at high temperatures. In order to evaluate the thermal stability of as-prepared composite membranes, a thermogravimetric analysis (TGA) was carried out under N_2 flow conditions from 50°C to 800°C . Figure 4 displays the TG and differential thermogravimetry (DTG) curves of the CS/TCNTs-0, CS/TCNTs-2, and CS/TCNTs-10 composite membranes. Because of the pretreatment of all the samples at 100°C , it is noted that there is no obvious weight loss caused by the removal of physically absorbed water, which is often observed in other chitosan-based membranes.²¹ All the as-prepared membranes show similar thermal degradation behavior, which can be clearly seen from the DTG curves [Figure 4(b)] in which there are two stages (two peaks) of fast thermal degradation. Because there are limited reports on the thermal stability of chitosan membranes crosslinked with sulfuric acid, it is difficult to ascertain the decomposition mechanism. However, with increasing TCNT content, the CS/TCNT composite membranes exhibit better thermal stability than that of a pure CS membrane under the same conditions. This can be explained by the fact that the fine dispersion of TCNTs in the CS matrix can increase the resistance of the membranes to thermal degradation, resulting in more gradual disintegration upon heating.

The oxidative stability is another key property for PEMs. Among the membrane degradation mechanisms, oxidative degradation is the most important factor because hydrogen peroxide and its decomposition products $\text{HO}\cdot$ and $\text{HOO}\cdot$ generated during fuel cell operation have strong oxidized characteristics. In order to evaluate whether the composite membrane could withstand a strong oxidizing environment during fuel cell operation, the oxidation stabilities of the membranes were compared by determining the time taken for samples to start to dissolve in a Fenton's solution at 80°C . The oxidation stability of the CS/TCNT composite membranes with different TCNT contents is shown in Figure 5. It is noted that the CS/TCNT composite membranes with a higher TCNT content exhibit better oxidative stability. For instance, the pure chitosan membrane begins to dissolve after just 111 min. The oxidation stability of the composite membranes improved significantly when adding TCNTs. The CS/TCNTs-2 composite membrane begins to dissolve after 181 min, while the CS/TCNTs-10 composite membrane begins to dissolve after 224 min, which is increased 101% over the pure chitosan membrane. This effective improvement of the oxidation stability of CS/TCNT composite membranes may be attributed to the excellent oxidation resistance of the TCNT constraint effect on the chitosan chains.

Water Uptake and Proton Conductivity of CS/TCNT Composite Membranes

The ability to take up water is very important for biopolymer membranes to be used in fuel cells. Generally, in the two widely

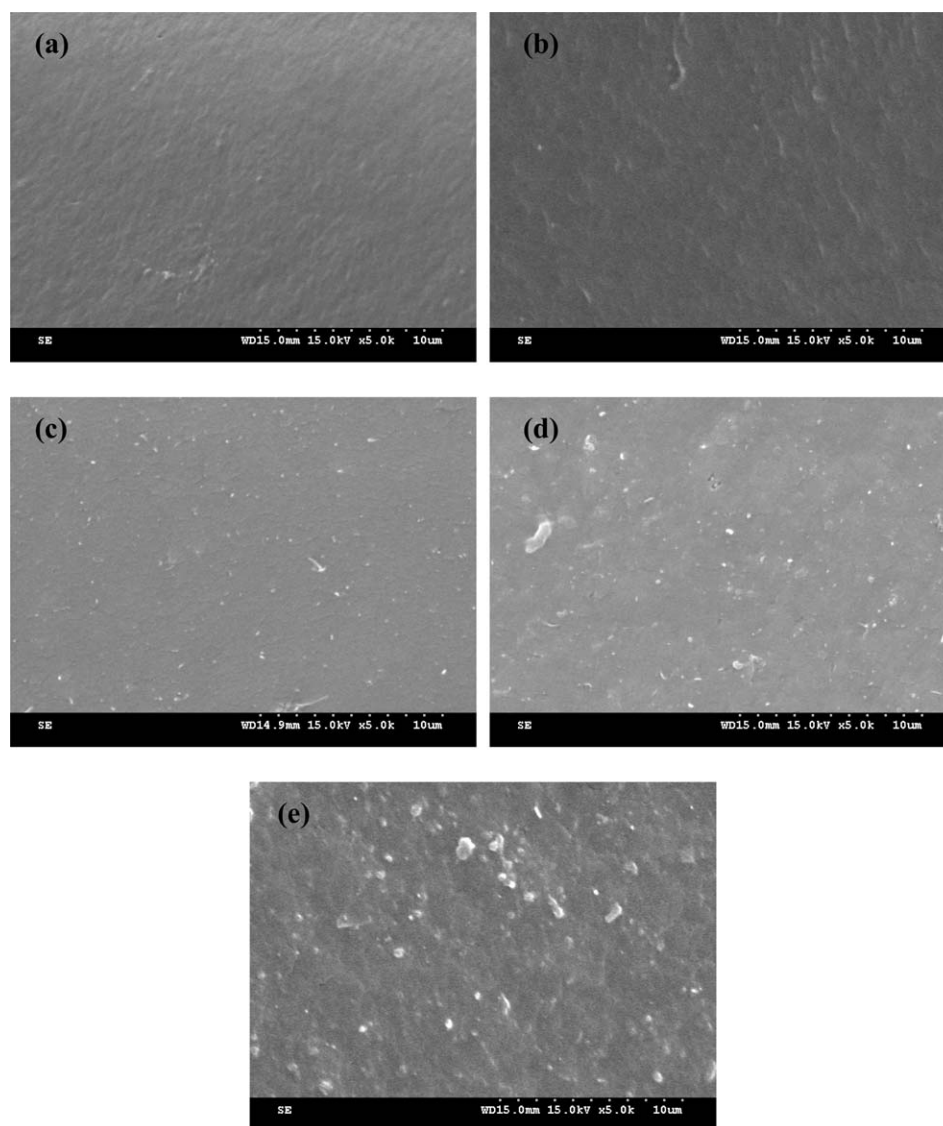


Figure 3. Cross-sectional SEM images of the composite membranes: (a) CS/TCNTs-0, (b) CS/TCNTs-1, (c) CS/TCNTs-2, (d) CS/TCNTs-5, and (e) CS/TCNTs-10.

accepted proton conduction mechanisms, the “Grotthuss” or “jump mechanism” and the “vehicle mechanism,” water is a vehicle for proton transfer in hydrated polymeric matrices by

electroosmotic drag and concentration-gradient-driven diffusion.²² The water uptake of the CS/TCNT composite membranes with different TCNT contents is shown in Figure 6. It is

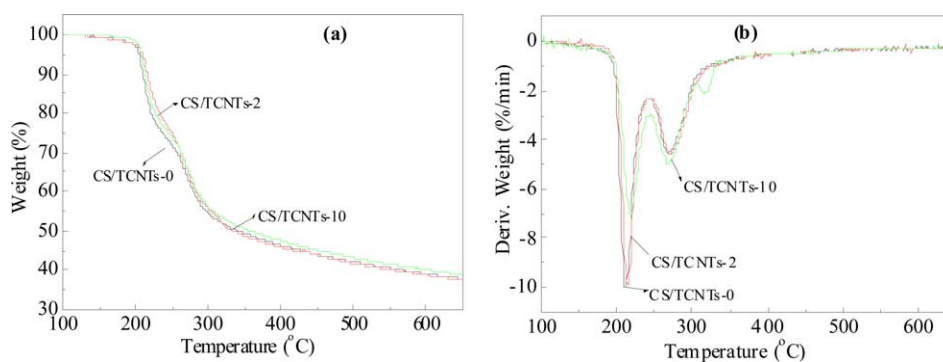


Figure 4. (a) TG and (b) DTG curves of CS/TCNT composite membranes. [Color figure can be viewed in the online issue, which is available at wileyonlinelibrary.com.]

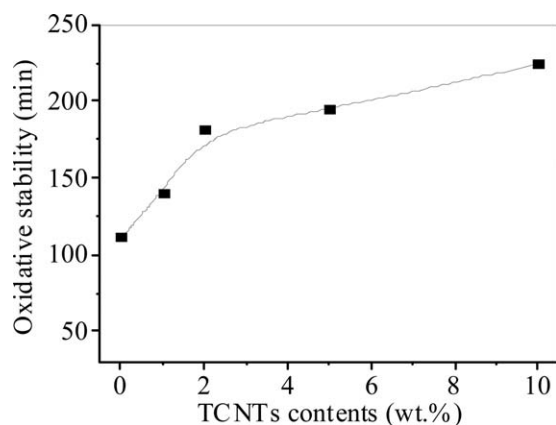


Figure 5. Oxidation stability of CS/TCNT composite membranes.

clearly seen that the water uptake of the composite membranes decreases with the increase of TCNT content. For instance, when the TCNT content increases from 1 wt % to 10 wt %, the water uptake of the composite membranes decreases from 124% to 74%. After reviewing the literature on chitosan and inorganic particle hybrids, we have reason to believe that there are two kinds of forces between chitosan and titania. One is an attractive force through the electrostatic interactions between the positively charged ammonium groups of the chitosan backbone and the negatively charged $-\text{TiOH}$. The other is the hydrogen bonds between the $-\text{TiOH}$ groups and the surface of TCNTs and the $-\text{OH}$ or $-\text{NH}_2$ groups of chitosan. Chitosan is a superhydrophilic natural polymer that possesses a large number of hydrophilic groups and can effectively combine with water molecules.^{23,24} After addition of TCNTs into the CS matrix, two kinds of forces between chitosan and titania as described above weaken the ability of the chitosan matrix to absorb moisture. Therefore, the water uptake of the CS/TCNT composite membranes decreased.

Proton conductivity is the foundation of PEM fuel cells. It is usually the most important characteristic considered when selecting membranes for potential fuel cell applications. Figure 7 shows the proton conductivity of the CS/TCNT composite membranes with different TCNT contents. For comparison purposes, the commercial Nafion 117 membrane was also characterized under the same conditions. The measured conductivity of the Nafion 117 mem-

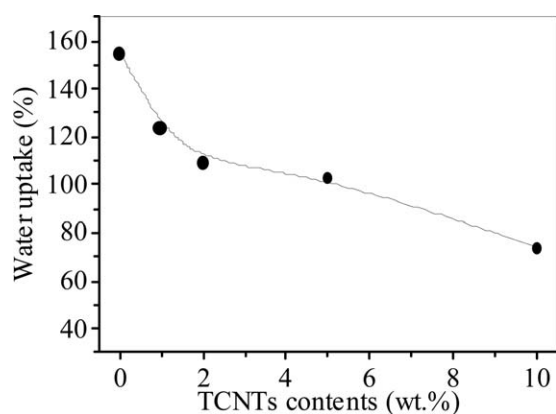


Figure 6. Water uptake of CS/TCNT composite membranes.

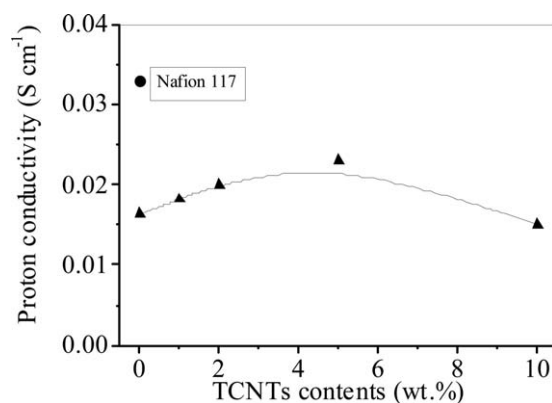


Figure 7. Proton conductivity of CS/TCNT composite membranes.

brane is 0.33 S cm^{-1} , which is slightly high but still close to the reported value.²⁵ The proton conductivity values of the CS/TCNT composite membranes increase as the TCNT content increases from 0 to 5 wt %. Subsequently, the proton conductivity values of the CS/TCNT composite membranes decrease when the TCNT content reaches 10 wt %. This change in proton conductivity may be attributed to the following reasons. When the TCNT content is no more than 5 wt %, in the fine dispersion of TCNTs in the chitosan matrix, the electrostatic interactions and hydrogen bonding interactions between them help to promote the formation of a continuous proton transport channel in the composite membranes. Moreover, the increased proton concentration, due to the decreased water dilution effect, is also responsible for the high proton conductivity because proton conductivity in a PEM depends on not only the effective proton mobility but also the proton concentration.²⁶ When the TCNT content reaches 10 wt %, the aggregation of TCNTs in the CS matrix increases the tortuosity of the proton-conducting pathway, and thus the proton conductivity decreases to some extent. However, the proton conductivity of CS/TCNT composite membranes is lower than that of the Nafion 117 membrane. It stays above $1 \times 10^{-2} \text{ S/cm}$, which is promising for applications in PEM fuel cells.

Mechanical Properties of CS/TCNT Composite Membranes

The mechanical properties affect the manufacturing conditions of the membrane electrode assembly and the durability of the PEM. Table I displays the mechanical properties of the Nafion 117 and CS/TCNT composite membranes with different TCNT contents. It is noted that the tensile strength and elongation at

Table I. Mechanical Properties of CS/TCNT Composite Membranes and Nafion 117 Membrane

Sample	Tensile strength (MPa)	Elongation at break (%)
CS/TCNTs-0	17.8 ± 0.25	234.7 ± 4.5
CS/TCNTs-1	20.4 ± 0.20	249.1 ± 4.0
CS/TCNTs-2	24.3 ± 0.30	286.2 ± 5.0
CS/TCNTs-5	29.0 ± 0.25	311.5 ± 4.5
CS/TCNTs-10	21.8 ± 0.20	197.0 ± 5.0
Nafion 117	27.1 ± 0.25	310.0 ± 4.0

break of the CS/TCNT composite membranes increase as the TCNT content increases but no more than 5 wt %. This result may be attributed to the fine dispersion of TCNTs in the CS matrix. The TCNTs play the role of a physics crosslinking point, which can restrain the mobility of the polymer chains under stress. Due to the aggregation of TCNTs in the CS matrix, the tensile strength and elongation at break of the CS/TCNT composite membranes decrease when the TCNT content was 10%. In addition, the tensile strength and elongation at break of the CS/TCNT composite membranes have already reached or are even better than that of the Nafion 117 membrane when the TCNT content reaches 5 wt %.

CONCLUSIONS

We have successfully prepared titania-coated carbon nanotubes (TCNTs) with a uniform titania layer on the surface of CNTs. The chitosan/TCNT (CS/TCNT) composite membranes were prepared by the solution casting method by stirring chitosan/acetic acid and a TCNT/ethanol suspension. The water uptake of the CS/TCNT composite membranes was reduced owing to the decrease of the effective number of the $-NH_2$ functional groups of chitosan. Due to the fine dispersion of TCNTs in the chitosan matrix, the thermal stability and mechanical properties of the CS/TCNT composite membranes were improved. The oxidation stability of the CS/TCNT composite membranes at 80°C in Fenton's reagent increased from 111 min to 224 min as the TCNT content reached 10 wt %. In addition, the proton conductivity of the CS/TCNT composite membranes increased from 0.016 S cm⁻¹ for CS/SCNT-0 to 0.023 S cm⁻¹ for CS/SCNT-5 on account of the electrostatic interactions and hydrogen bonding interactions between TCNTs and chitosan, helping to form the continuous ion transport channels. The results demonstrated that CS/TCNT composite membranes are promising materials for new proton-exchange membranes.

ACKNOWLEDGMENTS

This work was supported by funds from the National Natural Science Foundation of China (No. 51403058, 51303048, 31371750), Natural Science Foundation of Hubei Province (No. 2014CFB580), and by the faculty of Chemistry and Material Science, Hubei Engineering University.

REFERENCES

1. Ma, J.; Sahai, Y. *Carbohydr. Polym.* **2013**, *92*, 955.
2. Odeh, A. O.; Osifo, P.; Noemagus, H. *Energy Sources, Part A* **2013**, *35*, 152.
3. Vaghari, H.; Jafarizadeh-Malmiri, H.; Berenjian, A. *Sustainable Chem. Processes* **2013**, *1*, 16.
4. Pillai, C. K. S.; Paul, W.; Sharma, C. P. *Prog. Polym. Sci.* **2009**, *34*, 641.
5. Zhu, H. Y.; Fu, Y. Q.; Jiang, R. *Appl. Surf. Sci.* **2013**, *285*, 865.
6. Rungnim, C.; Ringrotmongkol, T.; Hannongbua, S. *J. Mol. Graphics Model.* **2013**, *39*, 183.
7. Domard, A. *Carbohydr. Polym.* **2011**, *84*, 696.
8. Marroquin, J. B.; Rhee, K. Y.; Park, S. *J. Carbohydr. Polym.* **2013**, *92*, 1783.
9. Tripathi, B. P.; Shahi, V. K. *Prog. Polym. Sci.* **2011**, *36*, 945.
10. Yang, J. M.; Chiu, H. C. *J. Membr. Sci.* **2012**, *419–420*, 65.
11. Kong, J.; Franklin, N. R.; Zhou, C. *Science* **2000**, *287*, 622.
12. Appenzeller, J.; Martel, R.; Derycke, V. *Microelectron. Eng.* **2002**, *64*, 391.
13. Jha, N.; Ramesh, P.; Bekyarova, E. *Sci. Rep.* **2013**, *3*, 2257.
14. Maiti, J.; Kakati, N.; Yoon, Y. S. *Solid State Ionics* **2011**, *201*, 21.
15. Kannan, R.; Kagalwala, H. N.; Pillai, V. K. *J. Mater. Chem.* **2011**, *21*, 7223.
16. Majedi, F. S.; Hasani-Sadrabadi, M. M.; Dashtimoghadam, E. *Phys. Status Solidi RRL* **2012**, *6(7)*, 318.
17. Blighe, F. M.; Hernandez, Y. R.; Blau, W. *J. Adv. Mater.* **2007**, *19(24)*, 4443.
18. Kilbride, B. E.; Coleman, J. N.; Fraysse, J. *J. Appl. Phys.* **2002**, *92(7)*, 4024.
19. Yamada, M.; Honma, I. *Electrochim. Acta* **2005**, *50*, 2837.
20. Mukherjee, R.; Sharma, R.; Saini, P. *Environ. Sci.: Water Res. Technol.* **2015**, *1*, 893.
21. Xiao, Y.; Xiang, Y.; Xiu, R. *Carbohydr. Polym.* **2013**, *98*, 233.
22. Wang, Y. B.; Yang, D.; Jiang, Z. Y. *J. Power Sources* **2008**, *183*, 454.
23. Rinaudo, M. *Prog. Polym. Sci.* **2006**, *31(7)*, 603.
24. Qin, C. Q.; Li, H. R.; Xiao, Q. *Carbohydr. Polym.* **2005**, *63*, 367.
25. Chen, W. F.; Wu, J. S.; Kuo, P. L. *Chem. Mater.* **2008**, *20(18)*, 5756.
26. Rodgers, M. P.; Shi, Z. Q.; Holdcroft, S. *J. Membr. Sci.* **2008**, *325*, 346.